International Academic Institute for Science and Technology

International Academic Journal of Science and Engineering
Vol. 12, No. 4, 2025, pp. 574-586.

ISSN 2454-3896

International Academic Journal of Science and Engineering

www.iaiest.com

Tribological Enhancement of Electroless Ni-P-TiO2 Coatings via Microwave Annealing

W. Anish [a], M. Edwin Sahayaraj [b*], S. John Leon [c], Lalu Gladson Robin [d], A.K. Darwins [e], B. Stanley Jones Retnam [f]

[a] Research Scholar, Noorul Islam Centre for Higher Education, Kumarakovil, Tamil Nadu, India. E-mail: anishlazar2018@gmail.com, Orcid: https://orcid.org/0009-0009-7147-766X
[b] Associate Professor, Automobile Engineering, Noorul Islam Centre for Higher Education, Kumarakovil, Tamil Nadu, India. E-mail: ebishaoun@gmail.com, Orcid: https://orcid.org/0009-0002-1729-3201*
[c] Associate Professor, Marine Engineering, Noorul Islam Centre for Higher Education, Kumarakovil, Tamil Nadu, India. E-mail: sjohnleon@gmail.com, Orcid: https://orcid.org/0009-0000-6655-5189
[d] Associate Professor, Automobile Engineering, Noorul Islam Centre for Higher Education, Kumarakovil, Tamil Nadu, India. E-mail: lalugrobin@gmail.com, Orcid: https://orcid.org/0000-0003-3178-6897
[e] Associate Professor, Automobile Engineering, Noorul Islam Centre for Higher Education, Kumarakovil, Tamil Nadu, India. E-mail: akdarwins@gmail.com, Orcid: https://orcid.org/0000-0002-9378-1656
[f] Associate Professor, Automobile Engineering, Noorul Islam Centre for Higher Education, Kumarakovil, Tamil Nadu, India. E-mail: bsjsjr@gmail.com, Orcid: https://orcid.org/0000-0001-5670-2376

Abstract

Microwave annealing is primarily used in polymer processing; however, in this study, it was successfully applied to a protective electroless Ni-P-TiO2 composite coating on low-carbon steel. The coated samples were annealed at various temperatures using both a conventional muffle furnace and a microwave furnace. Wear performance was evaluated using a pin-on-disc wear tester, while XRD and SEM analyses provided insights into phase transformations and the worn surface morphology of the coatings. Results indicated that the microwave-annealed coating exhibited significantly better wear resistance than the conventionally annealed coating, as evidenced by lower weight loss, a reduced coefficient of friction, and a lower specific wear rate.

Keywords: Electroless Coating, Nickel Composite Coating, Wear Resistance, Annealing, Microwave Annealing, Surface Modification.

DOI: 10.71086/IAJSE/V12I4/IAJSE12118
Received: 28 October 2025/Revised: 29 November 2025/Accepted: 17 December 2025/Published: 30 December 2025

Introduction

Metallic layers in aqueous solutions are mainly produced by electric current or chemical electron donors. The latter, electroless coating, introduced by Brenner and Riddle in the mid-20th century (Brenner & Riddell, 1946), does not require electric current, making it ideal for complex shapes and ensuring uniform deposition on any surface, whether metallic or non-conductive (Apachitei et al., 2002). Nickel-phosphorus alloy coatings are especially valued for their uniformity, hardness, self-lubrication, and wear and corrosion resistance, finding broad use in industries such as textiles, automotive, aerospace, and food processing (Staia et al., 1996; Sahayaraj et al., 2014; Sahayaraj et al., 2016 Leon et al., 2022).

Electroless Nickel (EN) coating is a selective plating process for low-alloy steels, aluminum, magnesium, and copper alloys. In this method, nickel ions are reduced with agents like sodium hypophosphite or sodium borohydride (Bonin et al., 2017; Leon et al., 2022; Loto, 2016; de Morais et al., 2024). The coating quality depends on the microstructure and composition of the deposits (Leon et al., 2018; Masoumi et al., 2012). EN coatings can be microcrystalline, amorphous, or crystalline, depending on their makeup. Heat treatment above ambient temperatures can alter microstructure, forming secondary Ni_xP_y phases that increase hardness, though excessive heating may reduce it over time (Yan et al., 2008; Palaniappa & Seshadri, 2008; Biswas et al., 2022; Biswas et al., 2016; Chintada et al., 2023; Chintada et al., 2022; Kumar et al., 2023).

EN composite coatings are widely used for abrasion-resistant applications. Nickel-phosphorus (Ni-P) coatings offer enhanced wear resistance with increased phosphorus content and heat treatment temperatures (Murali et al., 2022; Jekla, 2017; Chintada et al., 2022). Heat treatment generally improves coating hardness, boosting wear resistance, though excessive grain growth at high temperatures can reduce it (Dhakal et al., 2021; Liu et al., 2015; Rezaee et al., 2021; Yaghoobi et al., 2018). Various post-heat treatments, such as conventional furnace heating in air (Rabizadeh et al., 2010), inert atmospheres (Liu et al., 2012), vacuum heating (Novakovic & Vassiliou, 2009), laser (Liu et al., 2012; Hashemi & Shoja-Razavi, 2016; Arulvel et al., 2019), and plasma treatments (Tima & Mahboubi, 2021; Lin et al., 2013), have been explored to improve Ni-P coatings. However, research on microwave heat treatment for electroless nickel coatings remains limited.

Microwave heat treatment is increasingly recognized for its cost-effective, rapid, uniform, and selective heating advantages over traditional methods (Das et al., 2010). While commonly applied to areas like solar cell materials (Hart et al., 2007) and thin films (Simoes et al., 2007), our previous research demonstrated its potential to enhance the corrosion resistance of electroless nickel coatings (John et al., 2024; Sahayaraj et al., 2014). However, studies on the wear performance of microwave-treated EN coatings remain limited. This study prepared Ni-P/TiO_2 composite coatings and evaluated their wear performance in as-plated and heat-treated conditions using both microwave and conventional furnace methods at varying temperatures. The goal was to compare these treatments in terms of crystallinity and wear resistance, exploring whether microwave heating provides additional benefits for electroless composite nickel coatings.

Materials and Methods

Fabrication of Electroless Ni-P-TiO2 Composite Coating

Mild steel rods, annealed for 2 hours at 800°C for uniformity, were cut into 20 mm diameter and 3 mm thick samples. The surfaces were polished with various grades of emery sheets, pickled in 10% hydrochloric acid, and then rinsed with water and acetone. TiO_2 particles (200-300 nm, anatase, Merck) were manually spread (0.01 g) over the samples, which were placed in 20 mm x 6 mm glass beakers. The beakers containing the samples were then immersed in a plating bath (Table 1) to produce a Ni-P-TiO_2 composite coating.

Table 1: Plating Bath Constituent and Operating Condition

Constituent	Role	Quantity (g / l)
Nickel Chloride ($NiCl_2.6H_2O$)	Source of Nickel	30
Sodium Hypophosphite ($NaH_2PO_2H_2O$)	Reducing Agent	40
Sodium Citrate ($Na_3C_6H_5O_72H_2O$)	Stabilizer	30
Ammonium Chloride (NH_4Cl)	Complexing Agent	50
Operating Condition		
pH	9-10	
Temperature	82 (±1) °C	

Heat Treatment

Annealing of the coated samples was carried out using a conventional muffle furnace and a microwave furnace. The muffle furnace (Hasthas model) increased in temperature at 20°C/min, while the microwave furnace, operating at 2.45 GHz with a 10 kW Eurotherm PID controller, used a magnetron. Annealing treatment was conducted for one hour at temperatures between 300°C and 500°C.

XRD Measurement

Monochromatic Cu-Kα radiation was used for XRD measurements with a Siemens X-ray Diffractometer. Diffractograms showed variations in phases, grain sizes, and micro-strain in the deposits. The scans spanned a 2θ range of 10° to 90°, utilizing a 0.02° step size and a counting time of 2 seconds per step. Phases were identified using JCPDS files. Grain sizes and micro-strains were calculated using the Debye-Scherrer equation and Stokes-Wilson expression (Sahayaraj et al., 2014), respectively.

Wear Test

The wear resistance of the deposits was assessed using a Pin-on-Disc wear tester (Magnum Engineers, India, Pvt. Ltd.). A stationary pin sample, 30 mm in length, was tested against a rotating steel disc at a speed of 100 rpm, with a fixed wear track radius of 50 mm and an applied load of 5 N. Since the hardness of the coated surface exceeded that of the steel disc, a 220-grade emery sheet was placed over the disc (Apachitei et al., 2002) to facilitate wear between the coating and the silicon carbide particles in the emery sheet, preventing damage to the steel disc. The test was paused at intervals of 5, 10, 15, and 20 minutes to measure the weight loss and wear rate using the following equations.

$$\text{Specific Wear Rate} = \frac{\Delta V}{LD} \ (\text{mm}^3/\text{ N-m}) \quad (1)$$

Where,

Change of volume of the specimen (mm^3) $\Delta V = \frac{\Delta m}{\rho}$ (2)

Δm – Weight loss of the specimen (Initial weight – final weight) (g) (3)

Density of the deposited material (g/mm^3) $\rho = m / V$ (4)

m – Mass of the deposited material (g)

Volume of the coating material (mm^3) $V = A \times t$ (5)

A - Exposed Area of the specimen (mm^2)

t – Thickness of the coating in mm

L- Force applied on the specimen in N

D- Distance traveled by the specimen during the test in m.

Result and Discussion

Weight Loss

The weight loss during the wear test (sliding contact) was calculated using equation no. 3, with results for as-plated, conventional, and microwave heat-treated/annealed samples shown in fig 1A and 1B. These figures indicate that the as-plated Ni-P deposit experienced greater weight loss compared to heat-treated samples. This is likely due to its amorphous nature, which has lower hardness and higher ductility than annealed coatings (Zábranský et al., 2019). Additionally, weaker bonding between the TiO_2 particles and the coating may contribute to the increased weight loss in the as-plated coating.

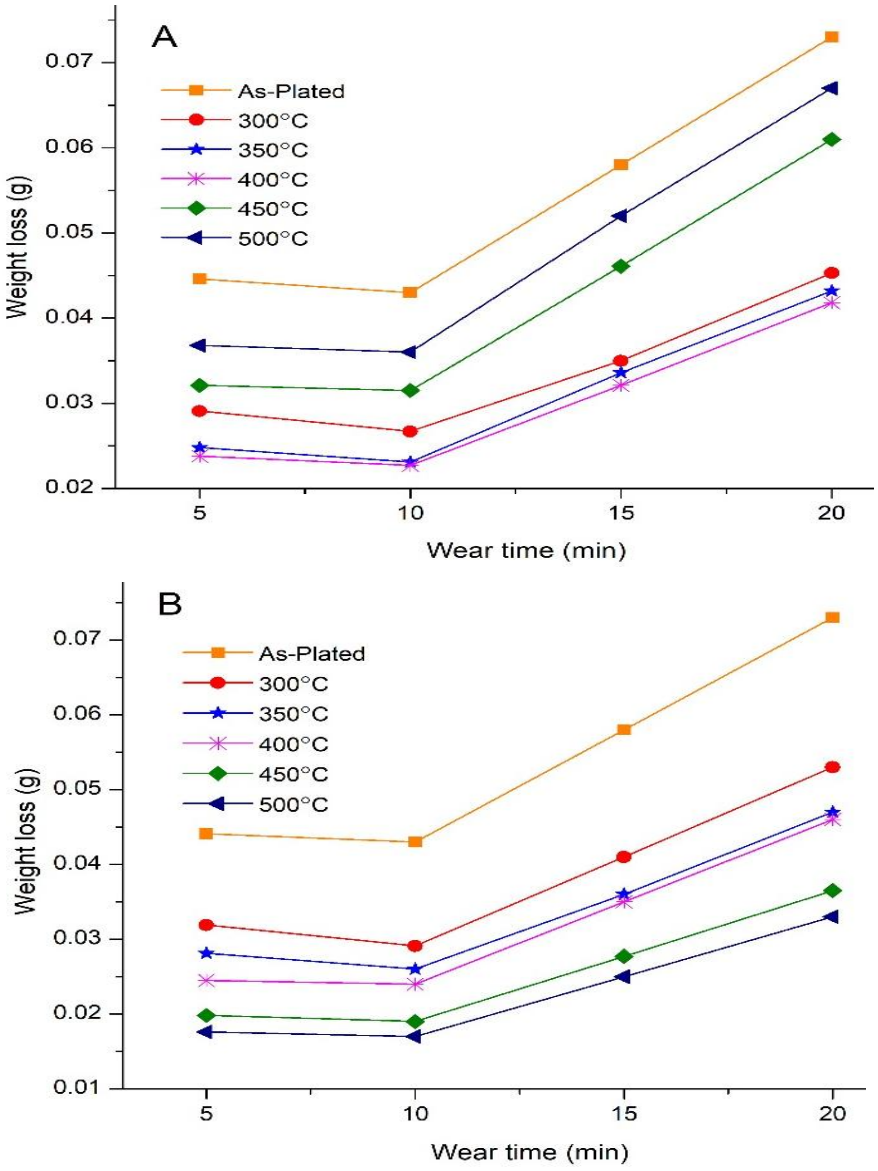


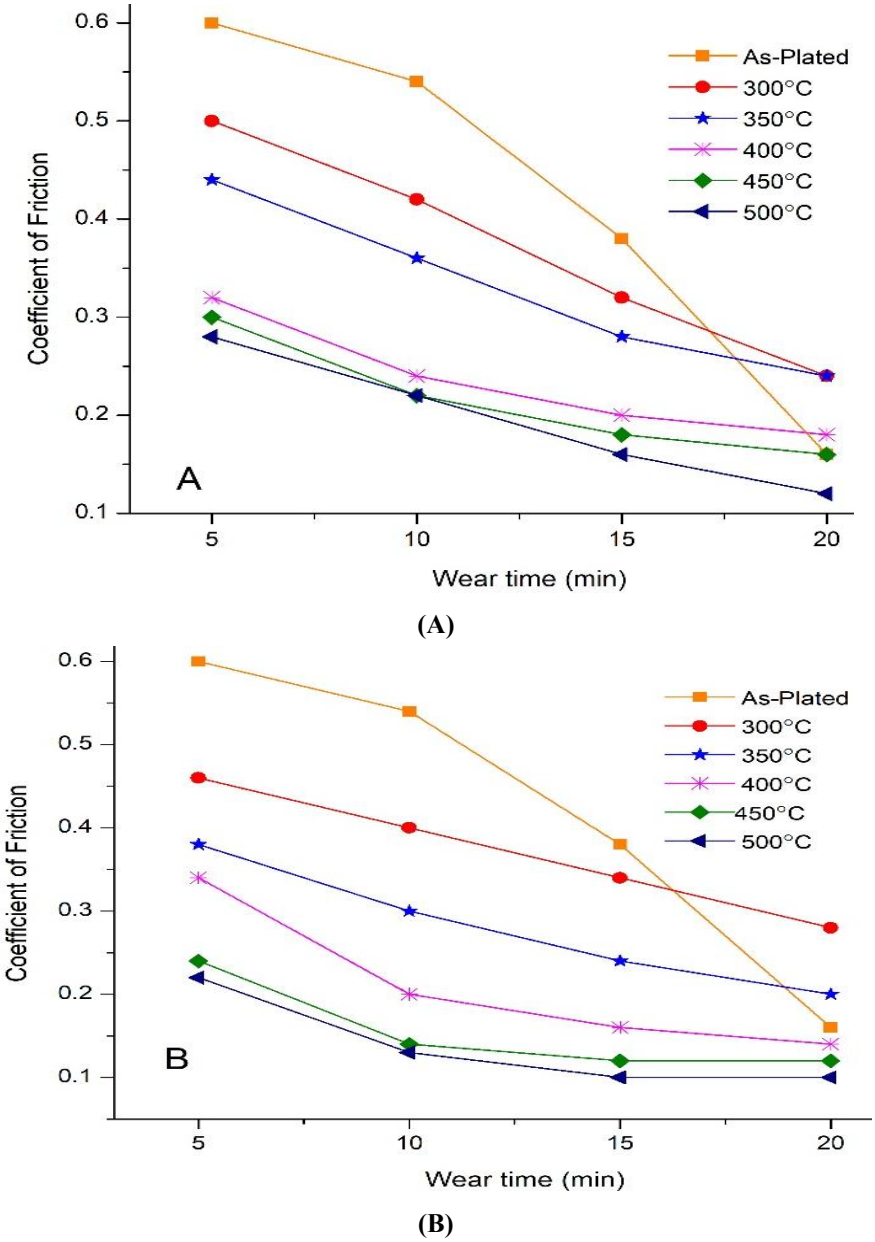
Fig. 1: Weight Loss of Coatings (A) Furnace Heat Treatment (B) Micro Wave Heat Treatment

Weight loss decreased with increasing annealing temperature up to 400°C for both muffle furnace and microwave methods. Conventional annealing showed lower weight loss than microwave annealing within this range. Above 400°C, weight loss increased with furnace annealing but decreased with microwave annealing. The lowest weight loss for conventional annealing was at 400°C, 127% higher than the minimum with microwave annealing at 500°C. The highest weight loss for microwave annealing was at 300°C, 126% lower than the maximum for conventional annealing at 500°C (after 20 minutes of sliding).

At lower microwave annealing temperatures (below 400°C), the incorporated TiO_2 particles absorb applied heat, reducing the recrystallization rate of Ni-P. This reduction limits the formation of secondary nickel-phosphorous phases, such as nickel phosphide, which would otherwise help to anchor the loosely bonded TiO_2 particles within the coating matrix. As a result, these particles are more easily removed during sliding, leading to higher weight loss. However, at higher annealing temperatures (above 400°C), grain boundary diffusion and accelerated molecular motion reduce cavities near TiO_2 particles, thereby enhancing bonding strength with the Ni matrix, as referenced in John et al., (2024) and Sahayaraj et al., (2014). This stronger bond minimizes TiO_2 particle detachment during sliding, reducing the coating's weight loss.

Coefficient of Friction

Fig 2A and 2B show the as-plated, conventionally annealed, and microwave-annealed electroless Ni-P-TiO_2 composite coatings. Initially, the coefficient of friction (COF) for the as-plated coating was high but gradually decreased over the first 10 minutes of sliding, followed by an abrupt drop. TiO_2 particles, embedded as clusters within the Ni matrix, projected above the surface, increasing hardness and surface roughness, which led to a higher COF at the start of sliding. As sliding continued, these clusters were pulled out, creating surface cavities. The dislodged particles became trapped between the mating surfaces, filling gaps between the SiC particles on the emery sheet, which improved lubrication and reduced the COF. After 10 minutes, further metal removal exposed the softer substrate, allowing it to contact the SiC, which further lowered the COF of the as-plated Ni-P-TiO_2 coating.



(A)

(B)

Fig. 2: Coefficient of Friction of Ni-P-TiO2 Composite Coating: (A) Conventional Furnace Annealing, and (B) Microwave Annealing, Compared with the As-Plated Condition

For both conventionally and microwave-annealed electroless Ni-P-TiO_2 composite coatings, the COF decreases as sliding contact time (wear time) increases. The COF curves for these coatings can be divided into three stages: stage I (5–10 min), stage II (10–15 min), and stage III (15–20 min). At the start of the wear test (stage I), the COF is

initially high but decreases gradually. This is due to the projection of embedded TiO_2 particles, which are harder and rougher than the coating material, onto the surface. Their hardness and roughness increase frictional force during sliding, thereby raising the COF initially.

In wear stage II, COF decreased for all annealing temperatures and methods, with the rate slowing as temperature increased. Up to 400°C, conventional annealing showed a slower COF decline than at higher temperatures, a trend also seen in microwave annealing. Above 400°C, the COF decrease was less pronounced in microwave annealing, likely due to microwave energy enhancing ionic movement, enabling nickel and nickel phosphide to fill boundary cavities. In stage III, COF gradually declined with increasing temperature below 400°C. Between 400°C and 450°C, conventional annealing showed minimal COF reduction, as the hardened coating blunted sharp SiC particles, ensuring smoother sliding. At 500°C, COF dropped sharply due to increased ductility, leading to higher material removal, weight loss, and substrate exposure, which reduced COF. In microwave annealing above 400°C, COF remained nearly constant in stage III, as stronger bonding, reduced weight loss, and increased hardness blunted SiC particles in stage II, preventing further COF changes.

Specific Wear Rate

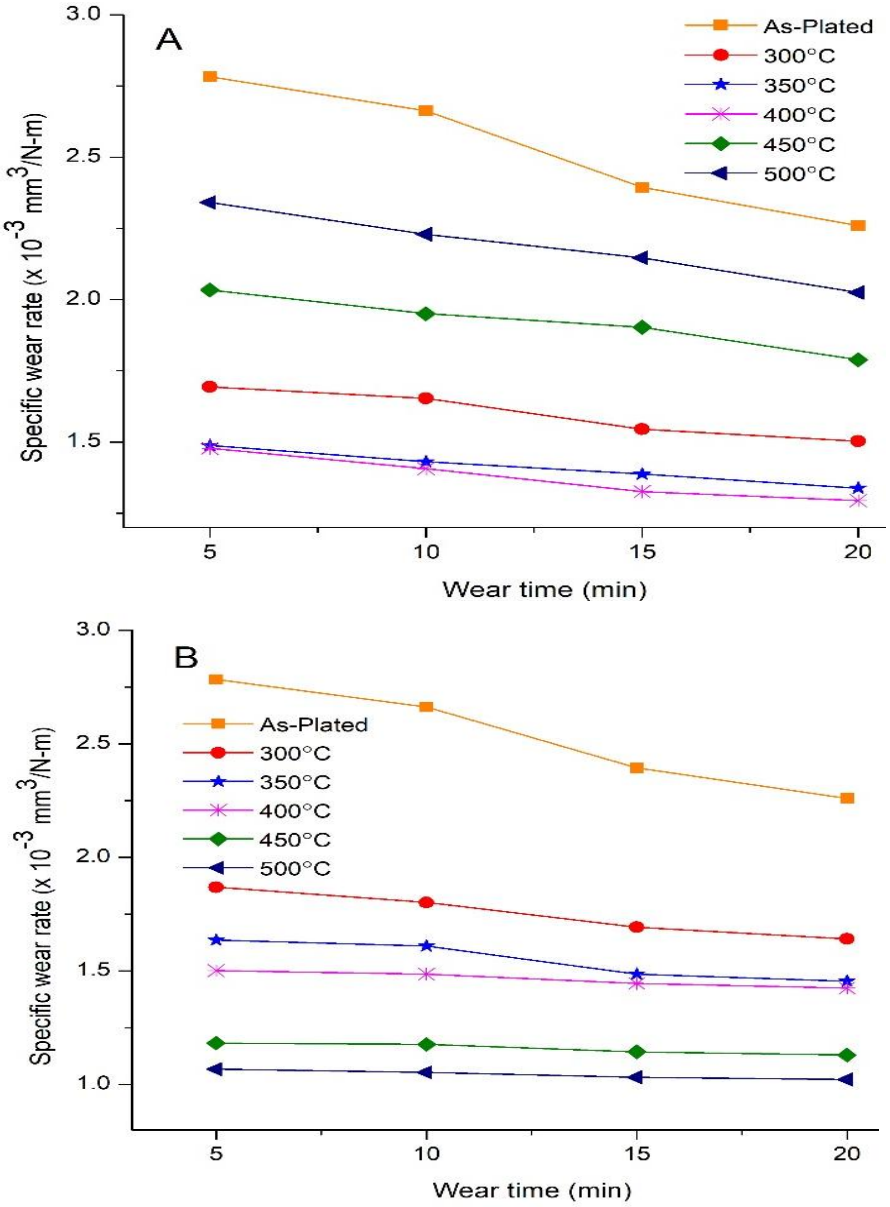


Fig. 3: Wear Rate of Friction of Coatings: (A) Conventional Heat Treatment. (B) Microwave Heat Treatment

The specific wear rate of the coating was calculated using equation 1, with a coating density of 7.65 x 10^{-3} g/mm^3 and a constant sliding velocity of 0.4 m/s. Fig 3A and 3B show the results for conventional and microwave annealed coatings, along with the as-plated coating. The as-plated coating had a higher wear rate than the annealed samples, likely due to its amorphous structure having lower hardness and no chemical bonding between the TiO_2 particles and the coating material. This resulted in weaker bonding strength compared to annealed coatings. The specific wear rate of the annealed coatings was lower than in the as-plated state due to crystallization during annealing, forming a hard Ni_3P phase that enhanced coating hardness and reduced wear, as shown in fig 4A and 4B.

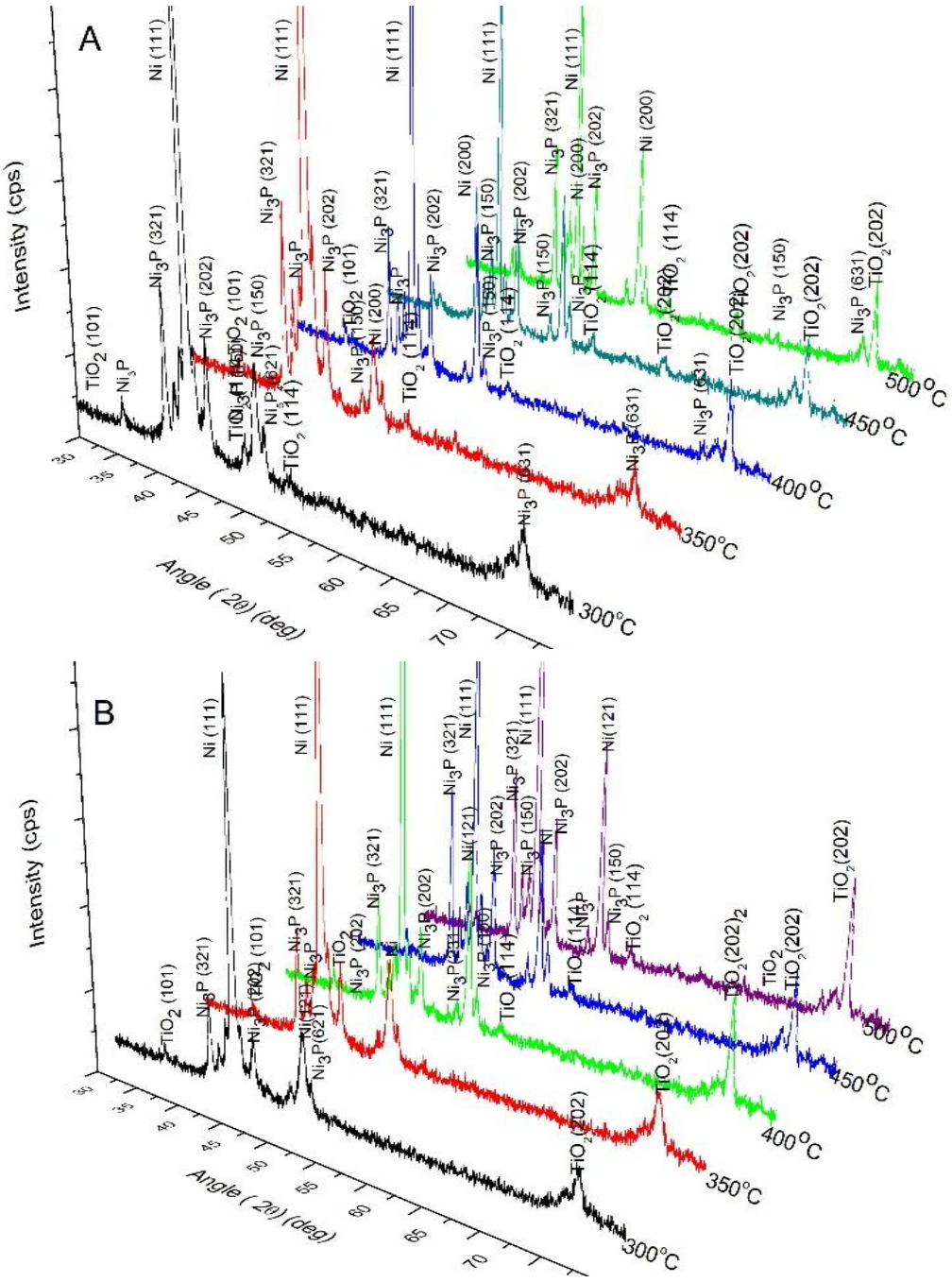


Fig. 4: XRD of Coatings: (A) Conventional Heat Treatment. (B) Microwave Heat Treatment

Fig 5A presents the worn surface morphology of the as-plated electroless Ni-P-TiO_2 composite coating. The worn surface reveals abrasive wear, caused by silicon carbide particles on the counter face. Small torn patches visible in the image indicate the removal of embedded TiO_2 particles, elongated along the wear direction, suggesting adhesive

wear. This observation supports the previously noted lower adhesive strength of the coating surface. Consequently, the Ni-P-TiO_2 coating experiences both abrasive and adhesive wear, with abrasive wear having a more pronounced effect on the wear rate than adhesive wear.

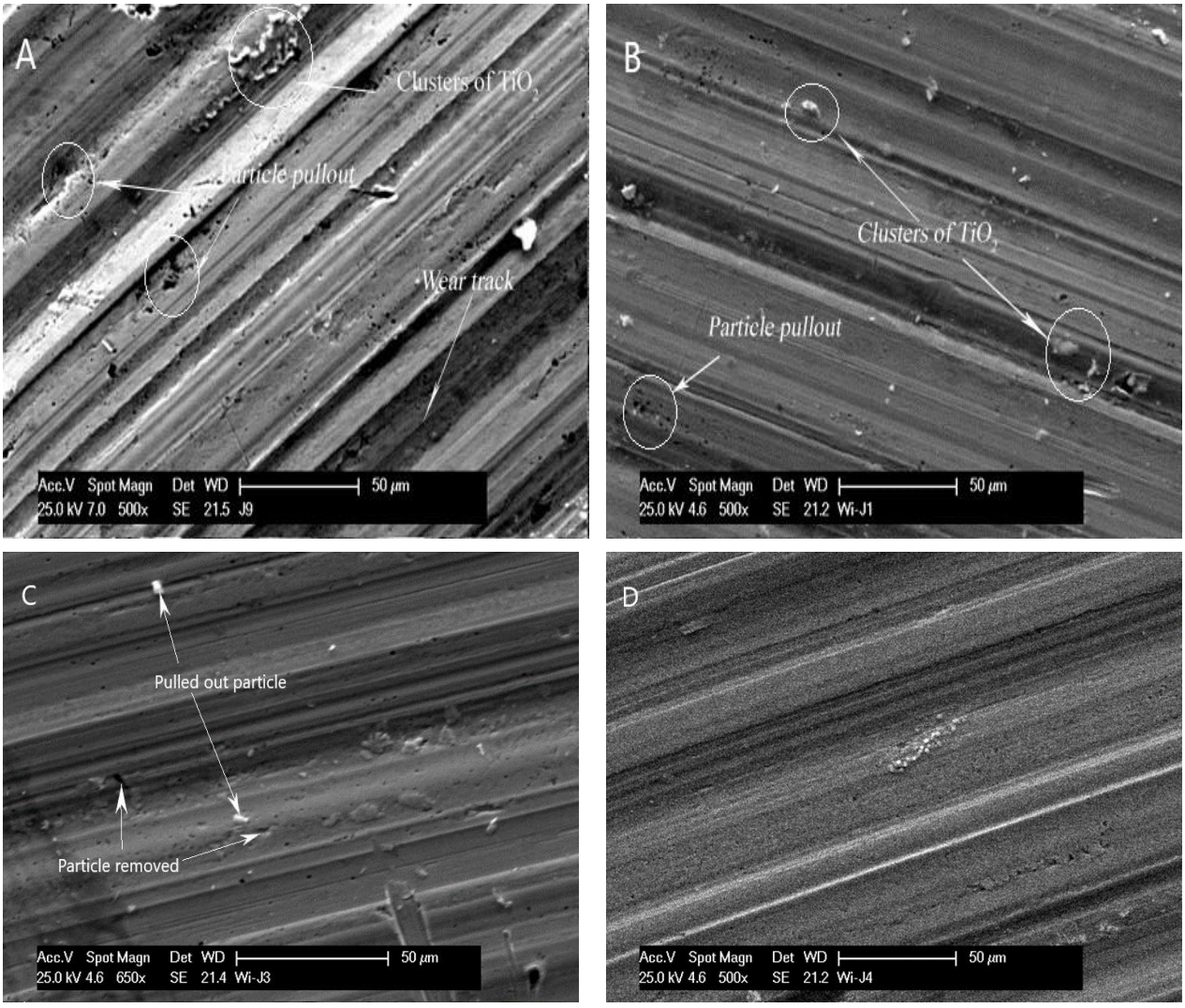


Fig. 5: Worn Surface Morphology of Ni-P-TiO2 Coating: (A) As-Plated, (B) Conventionally Annealed at 300°C, (C) 400°C, and (D) 500°C

Fig 5B, 5C, and 5D depict the worn surface morphology of conventionally annealed samples, showing smooth grooves and minor scratches indicative of predominant abrasive wear, with no adhesive wear. This results from the transformation of amorphous nickel into crystalline nickel and nickel phosphide, creating a denser matrix with securely embedded particles. Higher annealing temperatures reduce wear depth but widen wear tracks, enhancing coating smoothness and lowering friction. Bright spots in fig 5B - 5D represent TiO_2 particles dislodged during wear, adhering to the surface and causing scratches.

The lowest wear rate was observed at 400°C, where wear stabilized after the initial stage (Fig 3A), indicating coating integrity. This improvement is attributed to Ni_3P phase formation, which filled interfacial cavities around TiO_2 particles, enhancing adhesion and wear resistance. Fig 5C reveals particle chipping under the counter surface, with cavities from removed particles and clusters of TiO_2, suggesting partial coating retention. Beyond 400°C, wear increased due to Ni_3P phase coarsening, reducing Ni-Ni_3P solubility and interfacial bonding. Fig 5C and 5D show increased wear track width and depth, indicating greater material loss and possible substrate exposure, which, being softer, accelerated wear. At higher annealing temperatures, wear stage I had an initially high wear rate due to

protruding TiO_2 particles and sharp SiC counter surface particles increasing friction and weight loss. In stage II, friction and weight loss decreased, stabilizing wear with minimal changes into stage III.

The specific wear rate of microwave-annealed electroless Ni-P-TiO_2 composite coatings decreases as annealing temperature increases, as shown in fig 3B. Up to 400°C, microwave-annealed samples showed higher wear rates than furnace-annealed samples, but above 400°C, the wear rates were lower. Composite coatings were rougher than particle-free deposits due to TiO_2 particle entrapment during deposition, leaving some particle edges exposed and forming cavities that increased surface roughness. At lower microwave annealing temperatures, these cavities were not fully filled with Ni_3P phases, resulting in loosely bonded TiO_2 particles. During sliding, these particles chipped out easily, leaving black dots on the surface, as seen in SEM micrograph 6A. This effect was most pronounced at 300°C, with the highest wear rates. At 350°C, as shown in fig 6B, fewer cavities and improved Ni_3P formation led to stronger TiO_2 particle adherence, with slight protuberances indicating particle retention even after 20 minutes of sliding.

At 400°C, microwave annealing further reduces cavities in the coating and increases the number of protuberances compared to 350°C, as shown in fig 6C. The higher protuberance density correlates with a reduced wear rate above 400°C (Fig 6D). At 500°C, chipping effects diminish, and the wear track's width and depth decrease, leading to lower weight loss and a reduced coefficient of friction. Consequently, this coating exhibits the lowest wear rate among all annealed samples. In microwave annealing, wear rate is highest in stage I due to the fresh cutting edges of projected TiO_2 and SiC particles. However, a decreasing trend is observed at 300°C and 350°C during stages II and III. Beyond 400°C, the wear rate remains nearly constant after stage I (Fig 3B), likely due to improved adhesion strength, reduced porosity, and enhanced surface smoothness, lowering the coefficient of friction.

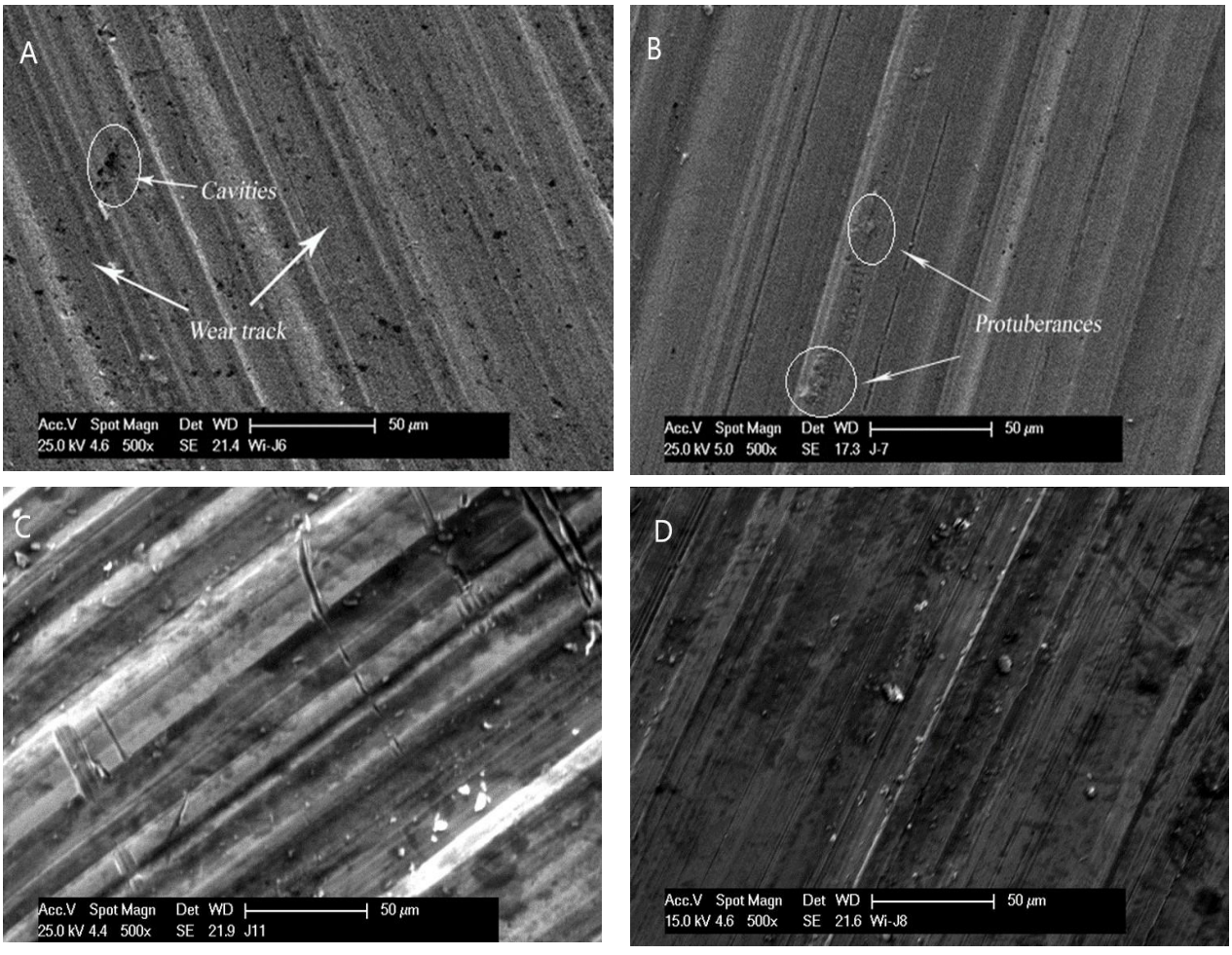


Fig. 6: Worn Surface Morphology of Microwave Annealed Ni-P-TiO2 Coating at (A) 300°C, (B) 350°C, (C) 400°C, and (D) 500°C

Microwave energy enhances molecular and ionic motion, which becomes vigorous above 400ºC, leading to diffusion. During this process, TiO_2 particles penetrate deeper into the coating, as observed by George et al., 2024 (John et al., 2024). Simultaneously, nickel ions diffuse into the substrate, while iron migrates upward, forming a strong nickel-iron inter-diffusion layer that securely retains TiO_2 particles during wear testing. EDS analysis of conventional and microwave-annealed Ni-P-TiO_2 coatings at 400°C (Fig 7A and 7B) confirms iron presence only in microwave-treated samples. This suggests that the inter-diffusion layer formed at ≥400°C enhances adhesion strength more than conventional annealing, thereby improving wear resistance.

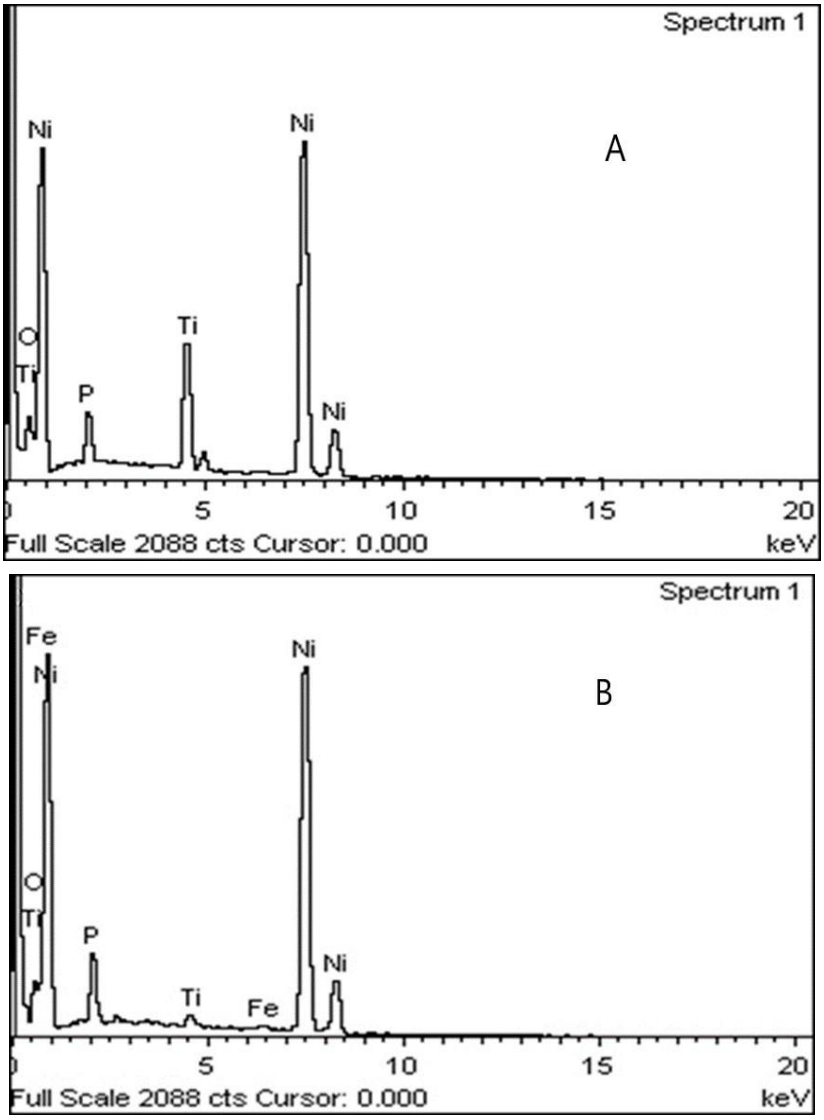


Fig. 7: EDS Spectrum of Ni-P-TiO2 Composite Coating Annealed at 400°C: (A) Conventional, (B) Microwave

Table 2: Elemental Weight Percentages in Conventionally and Microwave-Annealed Ni-P-TiO2 Composite Coatings

Elements (Wt. %)	Microwave Annealing Temperatures (ºC)			Conventional Annealing Temperatures (ºC)	
	300	400	500	400	500
Iron (Fe)	Nil	1.25	2.47	Nil	Nil
Nickel (Ni)	81.06	85.88	87.09	79.82	81.48
Phosphorous(P)	9.23	8.36	7.86	10.35	9.68
Titanium (Ti)	9.71	4.51	2.58	9.83	8.84

The elemental composition of the coatings annealed using microwave and conventional furnace treatments is presented in Table 2. Microwave annealing above 400°C increased diffused iron content, absent in conventional

annealing, which enhanced coating smoothness and likely reduced wear. At 500°C, the lowest wear rate for microwave annealing after 20 minutes of sliding was approximately 200% lower than conventional annealing at the same temperature and 127% lower than the best wear rate in conventional annealing. The highest wear rate for microwave annealing occurred at 300ºC, 117% higher than conventional annealing at the same temperature but 126% lower than the worst wear rate in conventional annealing. Overall, microwave annealing above 400ºC improved wear resistance more effectively than conventional annealing.

Conclusions

Ni-P-TiO_2 composite coatings were successfully prepared and annealed at various temperatures using conventional and microwave furnaces to evaluate wear performance. In both methods, Ni_3P phases formed, enhancing adhesion. The microwave annealing promoted ionic motion, enabling deeper diffusion of TiO_2 particles and coating elements while drawing iron from the substrate, improving smoothness and bonding strength. The lowest wear rate occurred at 500°C in microwave annealing, 127% lower than in conventional annealing. The highest wear rate at 300°C was still 126% lower than the worst in conventional annealing. Overall, microwave annealing above 400ºC significantly improved wear resistance compared to conventional annealing.

References

Brenner, A., & Riddell, G. E. (1946). Nickel plating on steel by chemical reduction. *Journal of research of the National Bureau of Standards*, *37*(1), 31-34. https://doi.org/10.6028/jres.037.019

Apachitei, I., Tichelaar, F. D., Duszczyk, J., & Katgerman, L. (2002). The effect of heat treatment on the structure and abrasive wear resistance of autocatalytic NiP and NiP–SiC coatings. *Surface and Coatings Technology*, *149*(2-3), 263-278. https://doi.org/10.1016/S0257-8972(01)01492-X

Staia, M. H., Castillo, E. J., Puchi, E. S., Lewis, B., & Hintermann, H. E. (1996). Wear performance and mechanism of electroless Ni- P coating. *Surface and coatings Technology*, *86*, 598-602. https://doi.org/10.1016/S0257-8972(96)03086-1

Sahayaraj, M. E., Jappes, J. W., & Siva, I. (2014). Effect of heat treatment temperature on the corrosion performance of electroless Ni-P/Ni-P-TiO2 deposits on carbon steel. *Journal of Advanced Microscopy Research*, *9*(1), 16-21. https://doi.org/10.1166/jamr.2014.1180

Sahayaraj, M. E., Jappes, J. W., Siva, I., & Rajini, N. (2016). Investigation on corrosion performance of multilayer Ni-P/TiO2 composite coating on steel. *Science and Engineering of Composite Materials*, *23*(3), 309-314. https://doi.org/10.1515/secm-2014-0134

Leon, S. J., Jappes, J. W., & Sahayaraj, M. E. (2022). Corrosion performance of annealed electroless Ni-B coatings on mild steel. *International Journal of Vehicle Structures & Systems*, *14*(3), 319-322. https://doi.org/10.4273/ijvss.14.3.06

Bonin, L., Bains, N., Vitry, V., & Cobley, A. J. (2017). Electroless deposition of nickel-boron coatings using low frequency ultrasonic agitation: Effect of ultrasonic frequency on the coatings. *Ultrasonics*, *77*, 61-68. https://doi.org/10.1016/j.ultras.2017.01.021

Loto, C. A. (2016). Electroless nickel plating–a review. *Silicon 8*, 177–186. https://doi.org/10.1007/s12633-015-9367-7

de Morais, A., Flacker, A., Hirata, M. K., Teixeira, R. C., & de Freitas, J. N. (2024). Electroless Ni–P plating deposited simultaneously on both surface sides of a flexible indium tin oxide coated polyethylene terephthalate substrate. *Journal of Materials Science: Materials in Electronics*, *35*(21), 1491. https://doi.org/10.1007/s10854-024-13228-6

Leon, S. J., Jappes, J. W., & Sahayaraj, M. E. (2018). Comparison of electroless Ni–P/Ni–B on corrosion performance. *International Journal of Engineering & Technology*, *7*(1.9), 88-92.

Masoumi, F., Ghasemi, H. R., Ziaei, A. A., & Shahriari, D. (2012). Tribological characterization of electroless Ni–10% P coatings at elevated test temperature under dry conditions. *The International Journal of Advanced Manufacturing Technology*, *62*(9), 1063-1070. https://doi.org/10.1007/s00170-011-3832-2

Yan, M., Ying, H. G., & Ma, T. Y. (2008). Improved microhardness and wear resistance of the as-deposited electroless Ni–P coating. *Surface and Coatings Technology*, *202*(24), 5909-5913. https://doi.org/10.1016/j.surfcoat.2008.06.180

Palaniappa, M., & Seshadri, S. K. (2008). Friction and wear behavior of electroless Ni–P and Ni–W–P alloy coatings. *Wear*, *265*(5-6), 735-740. https://doi.org/10.1016/j.wear.2008.01.002

Biswas, P., Das, S. K., & Sahoo, P. (2022). Evaluation of microhardness, wear, and corrosion behavior of duplex Ni–P/Ni–WP coatings. *Biointerface Research in Applied Chemistry*, *13*(5), 416.

https://doi.org/10.33263/BRIAC135.416

Biswas, A., Das, S. K., & Sahoo, P. (2016, September). Effect of heat treatment duration on tribological behavior of electroless Ni-(high) P coatings. In *IOP Conference Series: Materials Science and Engineering* (Vol. 149, No. 1, p. 012045). IOP Publishing. https://doi.org/10.1088/1757-899X/149/1/012045

Chintada, V. B., Gurugubelli, T. R., Tamtam, M. R., & Koutavarapu, R. (2023). Advancements in nickel-phosphate/boron based electroless composite coatings: a comprehensive review of mechanical properties and recent developments. *Materials*, *16*(18), 6116. https://doi.org/10.3390/ma16186116

Chintada, V. B., Gurugubelli, T. R., & Koutavarapu, R. (2022). An investigation over the effect of the reducing agent on the properties of the ZnO-reinforced Ni–P coatings. *Journal of Materials Science: Materials in Electronics*, *33*(2), 950-958. https://doi.org/10.1007/s10854-021-07366-4

Kumar, R., Singh, P. K., Saha, S., Mishra, S. K., Kumar, P., & Gobinath, R. (2023). Investigation of corrosive and mechanical behaviour of Ni-P doped coating by utilizing electroless method. *Materials Letters*, *349*, 134826. https://doi.org/10.1016/j.matlet.2023.134826

Murali, P., Gopi, R., Saravanan, I., Devaraju, A., & Karthikeyan, M. (2022). Wear and mechanical properties of electroless NiP and NiP-Silicon Carbide (SiC) composite coatings on En8 steel. *Materials Today: Proceedings*, *68*, 1707-1710. https://doi.org/10.1016/j.matpr.2022.08.364

Jekla, P. I. A. N. (2017). Heat treatment of electroless Ni-P layers on an austenitic stainless-steel substrate. *Heat Treatment*, *51* (3), 413–417.

Chintada, V. B., Koona, R., & Rao Gurugubelli, T. (2022). Investigation on microhardness and corrosion resistance of ZnO reinforced Ni-P composite coatings at various annealing temperatures. *Advances in Materials and Processing Technologies*, *8*(1), 945-958. https://doi.org/10.1080/2374068X.2020.1835017

Dhakal, D. R., Kshetri, Y. K., Gyawali, G., Kim, T. H., Choi, J. H., & Lee, S. W. (2021). Understanding the effect of Si3N4 nanoparticles on wear resistance behavior of electroless Nickel-Phosphorus coating through structural investigation. *Applied Surface Science*, *541*, 148403. https://doi.org/10.1016/j.apsusc.2020.148403

Liu, H., Yao, H. L., Thompson, G. E., Liu, Z., & Harrison, G. (2015). Correlation between structure and properties of annealed electroless Ni–W–P coatings. *Surface Engineering*, *31*(6), 412-419. https://doi.org/10.1179/1743294414Y.0000000422

Rezaee, B., Kermani, E., Ejlali, S., Biniyazan, F., & Soleimanimehr, H. (2021). Nanoparticle concentration and heat treatment effects on microstructure and tribological behavior of the Ni-P nanocomposite coating. *Advanced Journal of Science and Engineering*, *2*(2), 71-78. https://doi.org/10.22034/advjscieng21022071

Yaghoobi, M., Bostani, B., Asl Farshbaf, P., & Ahmadi, N. P. (2018). An investigation on preparation and effects of post heat treatment on electroless nanocrystalline Ni–Sn–P coatings. *Transactions of the Indian Institute of Metals*, *71*(2), 393-402. https://doi.org/10.1007/s12666-017-1169-8

Rabizadeh, T., Allahkaram, S. R., & Zarebidaki, A. (2010). An investigation on effects of heat treatment on corrosion properties of Ni–P electroless nano-coatings. *Materials & Design*, *31*(7), 3174-3179. https://doi.org/10.1016/j.matdes.2010.02.027

Liu, H., Guo, R. X., Liu, Y., Thompson, G. E., & Liu, Z. (2012). The effect of processing gas on corrosion performance of electroless Ni-WP coatings treated by laser. *Surface and Coatings Technology*, *206*(15), 3350-3359. https://doi.org/10.1016/j.surfcoat.2012.01.039

Novakovic, J., & Vassiliou, P. (2009). Vacuum thermal treated electroless NiP–TiO2 composite coatings. *Electrochimica Acta*, *54*(9), 2499-2503. https://doi.org/10.1016/j.electacta.2008.12.015

Liu, H., Guo, R. X., Viejo, F., & Liu, Z. (2012). Comparison of microstructure and residual stress characteristics of electroless Ni–W–P coatings annealed with a laser and a furnace. *Surface and Coatings Technology*, *206*(8-9), 2380-2387. https://doi.org/10.1016/j.surfcoat.2011.10.037

Hashemi, S. H., & Shoja-Razavi, R. (2016). Laser surface heat treatment of electroless Ni–P–SiC coating on Al356 alloy. *Optics & Laser Technology*, *85*, 1-6. https://doi.org/10.1016/j.optlastec.2016.05.018

Arulvel, S., Elayaperumal, A., & Jagatheeshwaran, M. S. (2019). Comparative study on the friction-wear property of As-plated, Nd-YAG laser treated, and heat treated electroless Nickel-Phosphorus/Crab shell particle composite coatings on mild steel. *Surface and Coatings Technology*, *357*, 543-558. https://doi.org/10.1016/j.surfcoat.2018.10.051

Tima, R., & Mahboubi, F. (2021). Effect of plasma nitriding temperature on microstructure and wear properties of electroless nickel-boron coatings. *Surface and Coatings Technology*, *415*, 127084. https://doi.org/10.1016/j.surfcoat.2021.127084

Lin, J. D., Kuo, C. L., & Hsia, C. J. (2013). The influence of microwave-assisted hydrogen plasma treatment on electroless Ni–P coatings. *Materials Chemistry and Physics*, *137*(3), 848-858.

https://doi.org/10.1016/j.matchemphys.2012.10.025

Das, S., Mukhopadhyay, A. K., Datta, S., & Basu, D. (2010). Evaluation of microwave processed glass–ceramic coating on nimonic superalloy substrate. *Ceramics International*, *36*(3), 1125-1130. https://doi.org/10.1016/j.ceramint.2009.12.003

Hart, J. N., Menzies, D., Cheng, Y. B., Simon, G. P., & Spiccia, L. (2007). A comparison of microwave and conventional heat treatments of nanocrystalline TiO2. *Solar energy materials and solar cells*, *91*(1), 6-16. https://doi.org/10.1016/j.solmat.2006.06.059

Simoes, A. Z., Riccardi, C. S., Ramírez, M. A., Cavalcante, L. S., Longo, E., & Varela, J. A. (2007). Synthesis and characterization of CaBi4Ti4O15 thin films annealed by microwave and conventional furnaces. *Solid State Sciences*, *9*(8), 756-760. https://doi.org/10.1016/j.solidstatesciences.2007.05.003

John, P. G., Sahayaraj, M. E., Jappes, J. W., & Leon, S. J. (2024). Corrosion characteristics of microwave and furnace annealed electroless Ni-P-TiO2 coatings. *Proceedings of the Institution of Mechanical Engineers, Part C: Journal of Mechanical Engineering Science*, *238*(4), 1149-1156. https://doi.org/10.1177/09544062231179086

Sahayaraj, M. E., Jappes, J. T. W., Siva, I., & Saravanan, M. S. S. (2014). A comparative corrosion study of electroless Ni-P coatings treated by microwave and conventional furnace annealing. *Corrosion Reviews*, *32*(1-2), 43-49. https://doi.org/10.1515/corrrev-2013-0052

Zábranský, L., Souček, P., Vašina, P., Dugáček, J., Sťahel, P., Buršík, J., ... & Buršíková, V. (2019). Microstructural changes of amorphous Mo–B–C coatings upon thermal annealing. *Surface and Coatings Technology*, *379*, 125052. https://doi.org/10.1016/j.surfcoat.2019.125052